ACS APPLIED MATERIALS & INTERFACES

RESEARCH ARTICLE

www.acsami.org

Gold Nano-Popcorn Attached SWCNT Hybrid Nanomaterial for Targeted Diagnosis and Photothermal Therapy of Human Breast Cancer Cells

Lule Beqa, Zhen Fan, Anant Kumar Singh, Dulal Senapati, and Paresh Chandra Ray*

Department of Chemistry, Jackson State University, Jackson, Mississippi, United States

ABSTRACT: Breast cancer presents greatest challenge in health care in today's world. The key to ultimately successful treatment of breast cancer disease is an early and accurate diagnosis. Current breast cancer treatments are often associated with severe side effects. Driven by the need, we report the design of novel hybrid nanomaterial using gold nano popcorn-attached single wall carbon nanotube for targeted diagnosis and selective photothermal treatment. Targeted SK-BR-3 human breast cancer cell sensing have been performed in 10 cancer cells/mL level, using surface enhanced Raman scattering of single walls carbon nanotube's D and G bands. Our data show that S6 aptamer attached hybrid nanomaterial based SERS assay is highly sensitive to targeted human breast cancer SK-BR-3 cell line and it will be able to distinguish it from other non targeted MDA-MB breast cancer cell line and HaCaT normal skin cell line. Our results also show that 10 min of photothermal therapy treatment by 1.5 W/cm^2 power, 785 nm laser is enough to kill cancer cells very effectively using S6 aptamer attached hybrid nanomaterials. Possible mechanisms for targeted sensing and operating principle for highly efficient photothermal therapy have been discussed. Our experimental results reported here open up a new possibility for using aptamers modified hybrid nanomaterial for reliable diagnosis and targeted therapy of cancer cell lines quickly.

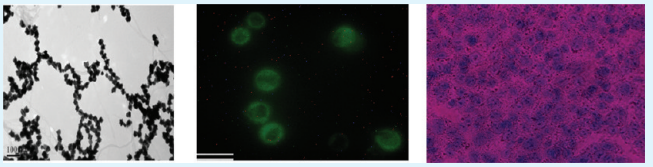

KEYWORDS: hybrid SWCNT, GNPOP, breast cancer, targeted cancer detection, SERS, targeted photothermal therapy

INTRODUCTION

Cancer has been described in early medical texts from antiquity, but it presents the greatest challenge in public health care in today's world.[1−10] Cancer is accounted for 13% of all worldwide deaths in 2007 and it is projected to continue rising, with an estimated 12 million deaths in 2030.[1−20] Breast cancer is the most common cancer among women and it is the second leading cause of cancer deaths in women today, after lung cancer.[1−20] The key to ultimately successful treatment of cancer disease is an early and accurate diagnosis.[1−25] Because of the unique structure of single wall carbon nanotubes (SWCNTs), there has been an explosion of interest in the use of SWCNTs for the development of biosensors.[25−42] Because of the presence of strong van der Waals interactions that tightly hold them together forming bundles, SWCNTs are insoluble in all solvents.[25−42] As a result, modification of SWCNTs using chemical functionalization is necessary to enhance solubility and produce novel hybrid materials that are potentially suitable for biosensing applications.[25−42] Typical Raman spectra of SWCNT consist of tangential Raman allowed optical mode E_{2g}, centered at 1590 cm^{-1} (G-band) and Raman band due to the defects, centered at 1340 cm^{-1} (D-band).[25−42] Normal Raman scattering is an inelastic scattering process of photons with matters. Because of its second-order dipole transition nature, the normal Raman signal is typically very weak.[8,43−55] Several articles reported that when molecules are adsorbed onto roughened surfaces or onto metal nanoparticles, the Raman signal is enhanced by several orders of magnitude because of the presence of collective oscillation of surface electrons on nanostructured materials.[8,43−55] Because of the established synthetic protocols for the controlled preparation of gold colloidal nanostructures and the presence of unique optical properties, gold nanomaterials have enormous potential in biology and medicine after functionalization with appropriate surface moieties.[8,43−70] In gold nano popcorn (GNPOP), like nanostar,[8,69,70] the central sphere acts as an electron reservoir while the tips are capable of focusing the field at their apexes. As a result, they are capable of providing enhancement of Raman signals by several orders of magnitude.[8,69,70] Using these unique properties of GNPOP and carbon nanostructure, in this article, we report design of novel hybrid nanomaterial based on GNPOP attached SWCNT as a SERS probe for targeted sensing of human breast cancer cells. For our study, a well-characterized human breast cancer cell line, SK-BR-3, which overexpresses the epithermal growth factor receptor HER2/c-erb-2/Neu (HER-2) on the cell surface[1−12] has been used to demonstrate the ultrasensitive detection capability. For SERS detection purpose, we have used Raman spectroscopic properties of individual SWCNT.[41,42] Since our SERS probe is free from dye labeling, this SERS probe will not suffer from photo bleaching problem. As a result, ideally, it has enormous potential for applications in cancer cell detection from clinical sample.

Current breast cancer chemotherapy treatment is often associated with severe side effects and as a result, new procedure that do not rely on traditional chemo therapeutic regimes, is very

Received: April 9, 2011
Accepted: August 15, 2011
Published: August 15, 2011

 © 2011 American Chemical Society

much in need for public health as well as world economy.[1−20] Recently published articles from several group including ours have demonstrated that gold nanoparticles of different sizes and shapes with tunable optical properties in the near-infrared (NIR) region can be exploited for the hyperthermic destruction of cancer cells.[8−17,51] Similarly, recently scientists have shown that SWCNT can be used as a drug in photothermal nanotherapy.[19−23,32−40] Both of them have the ability to generate high temperatures at a desired site which have been used for photothermal therapy of cancer cells. Using hybrid nanomaterial, one will be able to generate much higher temperature which will make photothermal process much more effective and fast. Also, SWCNT hybrid GNPOP is expected to have better biocompatibility and low toxicity. As a result, it will have greater promise for society for the therapeutic challenges of cancer. Driven by the need, in this article, we report for the first time the use of GNPOP-attached SWCNT hybrid nanomaterial-based photothermal therapy to kill the human cancer cell line selectively. Our experimental results have shown that 10 min of phototherapy treatment by 1.5 W/cm^2 power, 785 nm laser is enough to kill cancer cells very effectively. To demonstrate targeted detection and selective killing, we have also used HER2 negative human breast cancer MDA-MB cell line and human skin HaCaT keratinocytes, a normal skin line as a reference cell. Using an enzyme-linked immunosorbent assay kit, we found that the amount of HER2 in our SK-BR-3 cell was 6.3 × 10^6/ cells, whereas the HER2 amount was only 1.1 × 10^3/cells in the case of MDA-MB breast-cancerous cells. No HER2 was found in HaCaT cells.

MATERIALS AND EXPERIMENTS

Hydrogen tetrachloroaurate ($HAuCl_4.3H_2O$), $NaBH_4$, sodium citrate, SWCNT, and cetyl trimethylammonium bromide (CTAB) were purchased from Sigma-Aldrich and used without further purification. 3′-SH modified aptamers were purchased from Midland Certified Reagent. The human breast cancer cell lines were purchased from the American Type Culture Collection (ATCC, Rockville, MD). Human skin HaCaT keratinocytes, a transformed human epidermal cell line, was obtained from Dr. Norbert Fusenig of the Germany Cancer Research Center.

Synthesis of GNPOP. Our GNPOP synthesis was achieved through a two-step process, as we have reported recently.[8] In first step, very small, reasonably uniform, spherical seed particles were generated using trisodium citrate and sodium borohydride. In the second step, we have used ascorbic acid as a weak reductant as well as CTAB as a shape templating agent. JEM-2100F transmission electron microscope (TEM) and UV−visible absorption spectrum were used to characterize the nanoparticles (as shown in Figures 2 and 3). Concentration of GNPOP was determined using extinction coefficient 4.6 × 10^9 M^{-1} cm^{-1}, as we reported recently.[8]

Synthesis of GNPOP -Decorated SWCNT. We have synthesized GNPOP decorated SWCNTs using multi step process as shown in Figure 1A and discussed later in this manuscript. For the chemical design of label-free SERS probe, SWCNTs were attached to GNPOP through para-aminothiophenol, as shown in Figure 1A. For this purpose, chemical functionalization of SWCNT tips was performed mainly on the basis of oxidative treatments using 3:1 ratio of concentrated sulfuric acid and nitric acid.[24−42] Oxidation process yielded opened tubes with carboxylic acid functionality at both the sidewall and the tube endings.[24−42] After that, acid-chloride-functionalized SWCNTs were prepared by treating −COOH-functionalized SWCNTs with thionyl chloride in the presence of DMF catalyst under argon medium.[24−42] Figure 2B shows the TEM picture of acid chloride functionalized SWCNTs. After that, the acid chloride group was used as chemical anchors for further derivatization

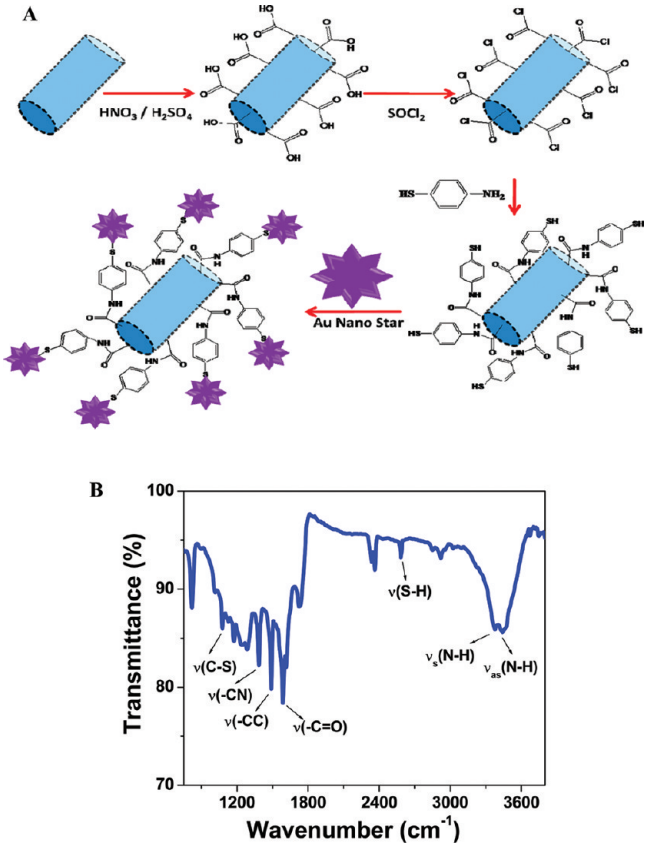

Figure 1. (A) Schematic representation shows the synthesis protocol for the formation of GNPOP attached SWCNTs. (B) FTIR spectra of aminothiophenol attached SWCNT.

with para-aminothiophenol, as shown in Figure 1A. At the end, GNPOP was attached with SWCNT through −SH linkage via aminothiophenol. Figure 2C shows the TEM picture of GNPOP conjugated SWCNT. Our data clearly show that the GNPOPs are nicely decorated on SWCNTs.

Synthesis of Aptamer-Conjugated, GNPOP-Decorated SWCNT. −SH-modifed aptamers were gradually exposed to GNPOP-decorated SWCNTs in the presence of 0.1 M NaCl in a PBS buffer over a 16 h period. To remove the unbound aptamers, we centrifuged the solution at 8000 rpm for 20 min, and the precipitate was redispersed in 2 mL of the buffer solution. We repeated this process three times. To measure the number of aptamer molecules in each GNPOP, we performed fluorescence analyses, as we reported before.[8] We estimated that there were about 150−200 aptamers per one GNPOP.

Fluorescence Analysis. Cancer cells were plated at a density of 1 × 10^5 cells/well and incubated for 24 h for cell attachment. After that, the cells were incubated for 1−4 h with Cy3 modified aptamers attached GNPOP modified SWCNT. They were then washed three times to remove unbound nanomaterial and a fresh cell culture medium was added. For fluorescence imaging, we used an Olympus IX71 inverted confocal fluorescence microscope fitted with SPOT Insight Digital Camera.

Cell Culture and Cellular Incubation with SWCNT Hybrid Nanoparticle. Cancer cells were grown in a 5% CO_2 incubator at 37 °C using RPMI-1640 medium (ATCC, Rockville, MD) supplemented with 10% premium fetal bovine serum (FBS) (Lonza, Walkersville, MD) and antibiotics (10 IU/mL penicillin G and streptomycin) in 75 cm^2 tissue culture flasks. An enzyme-linked immunosorbent assay kit was used to quantify HER2 in different tested cells. Our experimental results indicate that amount of HER2 in SK-BR-3 cells was 6.3 × 10^6/cells,

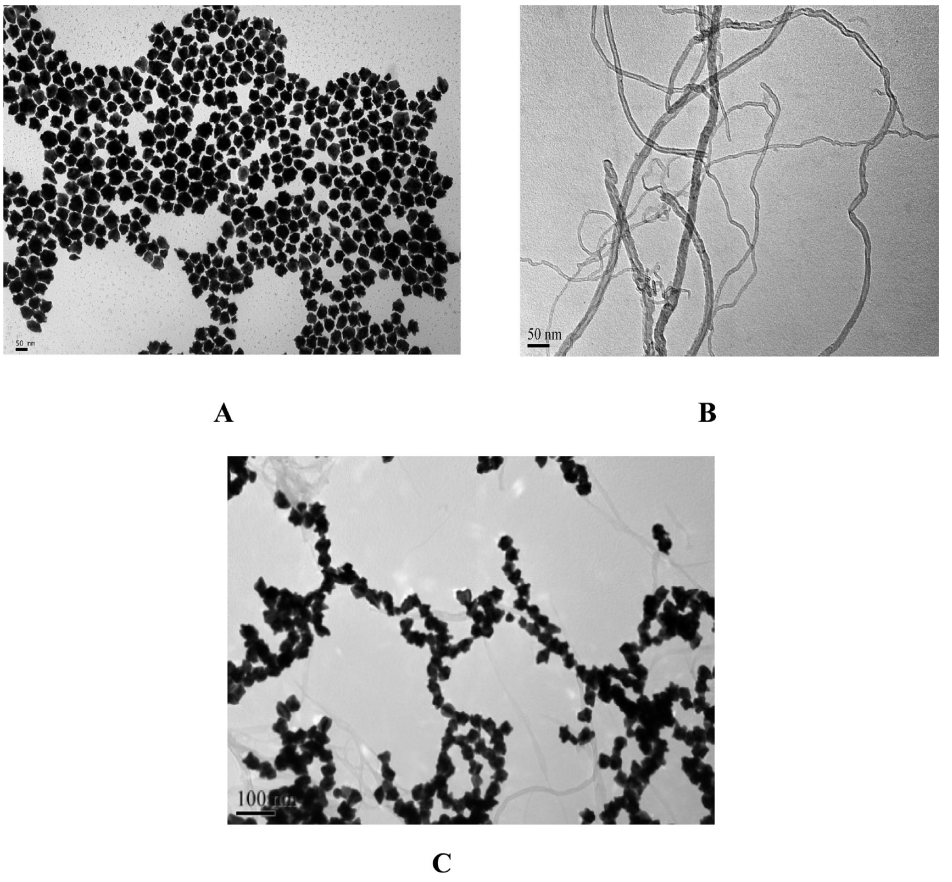

Figure 2. (A) TEM image showing freshly prepared GNPOPs. (B) TEM image showing acid chloride functionalized SWCNTs. (C) TEM image showing GNPOPs functionalized SWCNTs. In this case, we have used 10 μg/mL modified SWCNT and 1.5 nM GNPOP.

whereas HER2 amount was only 1.1×10^3/cells in the case of MDA-MB breast cancer cell. No HER2 has been observed for HaCaT cell line.

Surface-Enhanced Raman Spectroscopy (SERS) for Targeted Sensing of Cancer Cells. For SERS experiment, we have designed a SERS probe which we have reported recently.[8,45] In brief, we have used a continuous wavelength DPSS laser from laser glow technology (LUD-670) operating at 670 nm as an excitation light source. InPhotonics 670 nm Raman fiber optic probe has been used for excitation and data collection. It is a combination of 90 μm excitation fiber and 200 μm collection fiber with filtering and steering micro-optics. A miniaturized QE65000 scientific-grade Spectrometer from Ocean Optics has been used as a Raman detector, with spectral response range 220−3600 cm^{-1}. It is equipped with TE-cooled 2048 pixel CCD and interfaced to computer via a USB port.

Photothermal Therapy and Percentage of Live Cell Determination. For photothermal therapy experiment, we have used a continuous wavelength portable OEM laser operating at 785 nm, as an excitation light source for 10−20 min. After that, we have used MTT test to find the amount of live cells during nanotherapy process. For this purpose, breast cancer cells were seeded in 96-well plates (well diameter 6.4 mm) with a density of 100,000 cells/well and allowed to attach for 24 h at 37 °C in a 5% CO_2 incubator, before the treatment. After incubation, the cell monolayer in the wells was repeatedly rinsed with PBS buffer to remove the nonspecifically adsorbed nanomaterials remaining in the medium and then was exposed to the laser at 785 nm. Cell viability was also determined 1 h after photothermal treatment using the 3-(4, 5-dimethylthiazol-2-yl)-2,5-diphenyltetrazolium bromide (MTT) cell proliferation assay kit (ATCC CA# 30−1010k). This experiment has been performed 5−6 times and average values are reported in this manuscript.

RESULTS AND DISCUSSIONS

For the chemical design of hybrid nanomaterial, SWCNTs were attached to GNPOP through para-aminothiophenol, as shown in Figure 1A. For this purpose, chemical functionalization of SWCNT tips was performed mainly on the basis of oxidative treatments using 3:1 ratio of concentrated sulfuric acid and nitric acid.[24−42] Oxidation process yields opened tubes with carboxylic acid functionality at both the sidewall and the tube endings.[24−42] After that, acid chloride functionalized SWCNTs were prepared by treating −COOH functionalized SWCNTs with thionyl chloride in presence of DMF catalyst under argon medium.[24−42] Figure 2B shows the TEM picture of acid chloride functionalized SWCNTs. In next step, the acid chloride group was used as chemical anchors for further derivatization with para-aminothiophenol, as shown in Figure 1A. Now to understand whether aminothiophenol has been attached with SWCNT or not, we have performed FTIR spectra. As shown in Figure 1B, we have seen clearly all the characteristic peaks for aminothiophenol[71] and these are -SH and −CS stretching vibrations at 2524 and 1088 cm^{-1} respectively. The absorption peak at 1306 cm^{-1} is a −CN stretching vibration. The 3448 cm^{-1} peak is an -NH asymmetrical stretching vibration and the one at 3359 cm^{-1} is the symmetrical stretching vibration of −NH. All the other peaks are mainly due to the SWCNT, −C═O, and −C═C− stretching

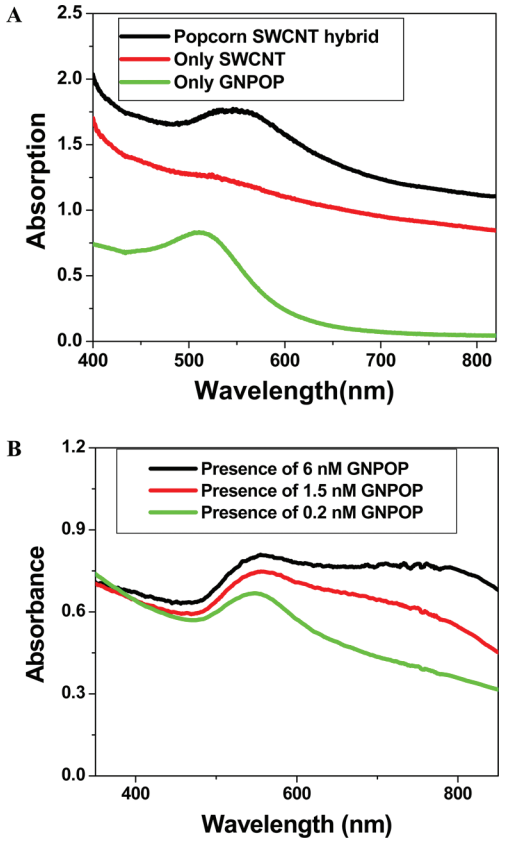

Figure 3. (A) Absorption spectra for 0.2 nM GNPOP, 10 μg/mL modified SWCNT and 0.2 nM GNPOP attached SWCNT. The strong long wavelength band in the visible region (λ_{PR} = 550 nm) is due to the oscillation of the conduction band electrons of GNPOP. B) Absorption spectra for GNPOP attached SWCNT with different concentrations of GNPOP. In all cases, we have used 10 μg/mL modified SWCNT.

vibration bands of aminothiophenol.[71,72] Because free thiol group is available for linkage with gold nanoparticle and it is very well-known that thiol group strongly stabilizes gold nanoparticle though Au−S bond, GNPOP was attached with SWCNT using −SH linkage via aminothiophenol, as shown in Figure 1A. After functionalization, free gold nanoparticles were separated after centrifuging the mixture at 4000 rpm for 30 min. Figure 2C shows the TEM picture of GNPOP-conjugated SWCNT. Our data show that the GNPOPs are nicely decorated on SWCNTs. Figure 3A shows the absorption spectra of only SWCNT, 0.2 nM GNPOP and 0.2 nM GNPOP attached SWCNT. Broad and structureless absorption spectrum from near-infrared and visible region from 400 to 850 nm is mainly due to the E_{11} and E_{22} transitions of nanotubes.[24−42] As shown in Figure 3A, in the case of GNPOP, we observed a strong long wavelength plasmon band around 550 nm that is due to the oscillation of the conduction band electrons.[8]

When we attached 0.2 nM GNPOP with 10 μg/mL SWCNT, the absorption spectrum seems like from the mixture of both, as shown in Figure 3A. Only change we observed is that the λ_{max} of GNPOP shifted slightly red, by about 10 nm and it is mainly due to the bond formation. Figure 3B show how the absorption spectra for SWCNT hybrid popcorn-shaped gold nanomaterial vary with the concentration of nanoparticles. Our experimental results show that as the concentration of GNPOP increases, the absorption spectra shift toward higher wavelength and become broad. It is mainly due to the fact that as we increase the concentration of nanoparticle, GNPOPs are very closely packed on SWCNT as shown in Figure 2C. As a result, the absorption band shifts to higher wavelength, because of the interparticle interaction and change in the local refractive index on the nanoparticle surface.

For the selective detection of targeted cancer cells, we modified the gold nanoparticle decorated SWCNTs with SK-BR-3 breast cancer cell specific S6 aptamers, as shown in Figure 4A.[8,12] Before performing the experiment with cancer cells, we have verified that our hybrid SWCNT is stable in buffer solution between pH 5−9 and also in serum for several hours. Our chemically designed GNPOP attached SWCNT hybrid nanomaterial based SERS approach for the detection of selective human breast cancer cell line is based on the fact that in the presence of SK-BR-3 cell line, S6 aptamer-conjugated, GNPOP-attached SWCNTs undergo aggregation (as shown in Figure 4B) due to the S6 aptamer cancer cell interaction. For SK-BR-3 breast cancer cell line, a cancer cell has several epithermal growth factor receptors HER2/c-erb-2/Neu (HER-2), which are available for specific recognition with S6 aptamer-conjugated, GNPOP-attached SWCNTs. As shown in Figure 4B, our TEM image shows S6 aptamers conjugated GNPOP decorated SWCNT aggregates on the surface of cancer cell. As a result, a new, very broad band appears around 160 nm far from their plasmon absorption band, as shown in Figure 4C. To understand better about the binding of aptamer modified nanomaterial with SK-BR-3 cell and also its selectivity, we have also performed fluorescence imaging analysis. For this purpose, we have used Cy3-modified, S6 aptamer-attached, GNPOP-modified SWCNT. About 1 million of SK-BR-3 cancer cells were incubated for 1 h with Cy3-modified nanomaterial. After that, we washed three times to remove unconjugated Cy3 attached nanoparticle. To decrease the autofluorescence signal, 488 nm light was selected for the excitation. As shown in Figure 5, confocal fluorescence imaging showed that the targeted Cy3 attached aptamer conjugated nanomaterials bind only with SK-BR-3 cells and do not bind with HER2 negative MDA-MB cells. We have observed the same result for HaCaT cells. So our results clearly show that S6 aptamer-attached, GNPOP-modified SWCNT is highly selective for binding with SK-BR-3 cell lines that overexpress HER2. Because of the formation of aggregates in the presence of SK-BR-3 cells, it formed several hot spots, which provided a significant enhancement of the Raman signal intensity from SWCNTs by 3 orders of magnitude through electromagnetic field enhancements, as shown in Figure 6. For SERS experiment, we have used a SERS probe using a continuous wavelength DPSS laser operating at 670 nm and miniaturized QE65000 Scientific-grade spectrometer as the Raman detector.[8,55]

As shown in Figure 6A, our SERS spectrum shows two clear SWCNT characteristic Raman bands between 1000 to 1650 cm^{-1} and these are: disorder related mode (D band) around 1300 cm^{-1} and tangential graphite-like mode (G band) around 1590 cm^{-1}. As shown in Figure 6A, Raman intensity of SWCNT bands increases by an order of magnitude once SWCNT has been decorated with GNPOP. Largest Raman scattering enhancements can be obtained for molecules, when it resides in the fractal space between aggregated colloidal nanoparticles, known as "hot spots".[8,43−55] Our TEM and fluorescence imaging data show that SK-BR-3 cancer cells help to generate hot spots through aggregation and as result, we have noted enhancement of 3 orders of

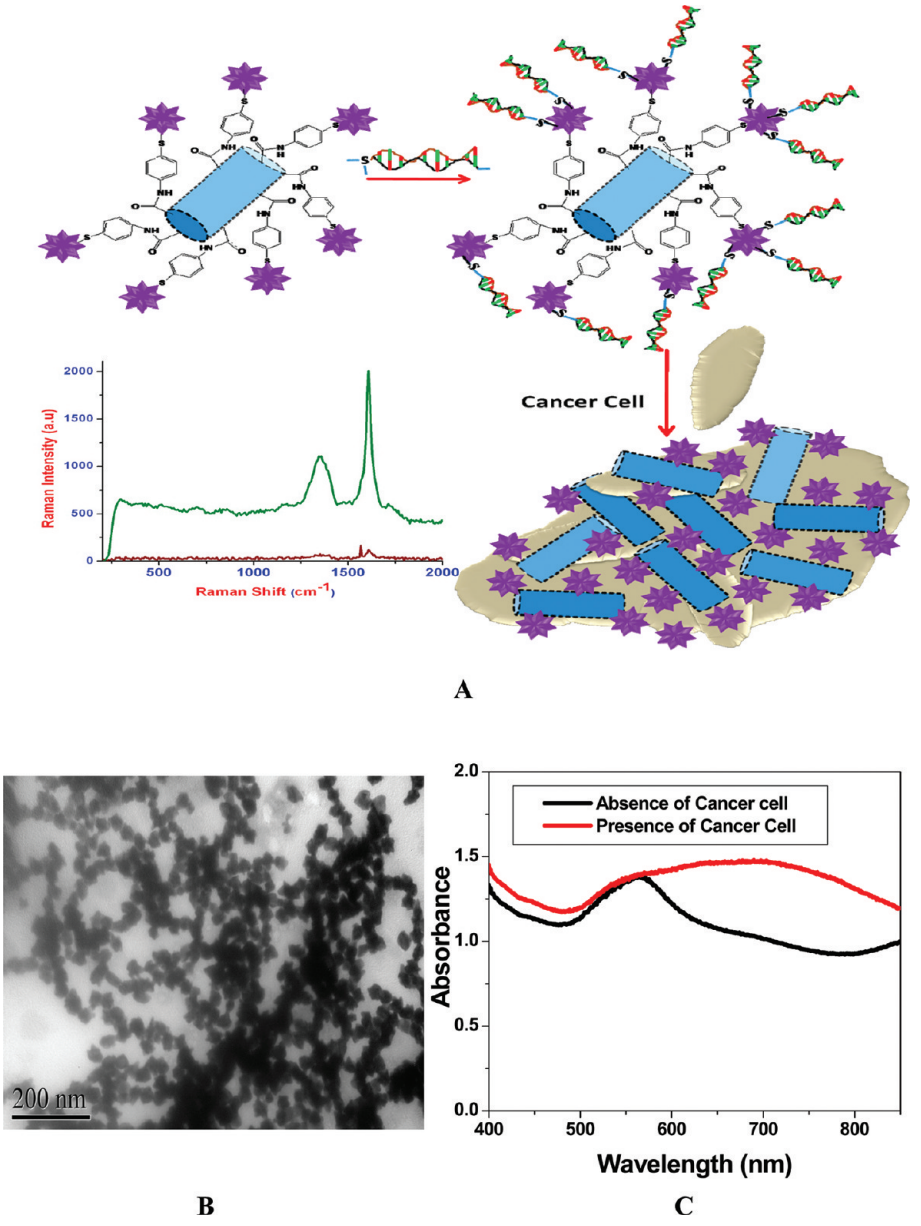

Figure 4. (A) Schematic representation shows SERS-based cancer cell detection using aptamer-attached, GNPOP-modified SWCNT. (B) TEM image shows aggregation of aptamer-conjugated, GNPOP-functionalized SWCNTs on cancer cell surface. (C) Absorption profile showing variation of absorption spectra of bioconjugated SWCNT hybrid GNPOPs due to the addition of SK-BR-3 cancerous cells. In this case, we have used 10 μg/mL modified SWCNT and 1.5 nM GNPOP hybrid.

magnitude of SWCNT G band Raman signal (as shown in Figure 6). To demonstrate that the assay is highly selective, we have also performed how SERS intensity changes upon the addition of HER2 negative human breast cancer cell line (MDA-AB). As we have discussed before, our fluorescence data show that the HER2 negative human breast cancerous MDA-MB cells are poorly labeled by the S6 aptamer-conjugated, GNPOP-decorated SWCNTs even after 4 h of incubation. As a result, we have not observed any significant SERS enhancement (as shown in Figure 6B) even after the addition of 1×10^5 MDA-MB cells. On the other hand, as shown in Figure 6B, we see significant SERS intensity change even after the addition of only 10 SK-BR-3 cells. Because of the lack of strong interaction, nanoparticles do not produce enough hotspots in case of MDA-MB cancer cell and as a result, significant SERS enhancement has not been observed. We have also observed similar result for HaCaT normal skin cell, where due to the lack of HER2, nanoparticles do not aggregate and as a result, significant SERS enhancement has not been observed, as shown in Figure 6B. This contrast difference clearly shows that our SWCNTs based label-free SERS assay is highly specific for HER2 human breast cancer cell line and even it can distinguish between-different breast cancer cell lines.

After successful targeted sensing, we have performed NIR irradiation experiments to determine whether hybrid nanomaterial can be used for photo thermal therapy of SK-BR-3 cancer cells. Before performing photothermal experiment, we have tested cytotoxicity of hybrid nanomaterial. For this purpose, we have incubated hybrid nanomaterial with SK-BR-3 cell for 24 h. And

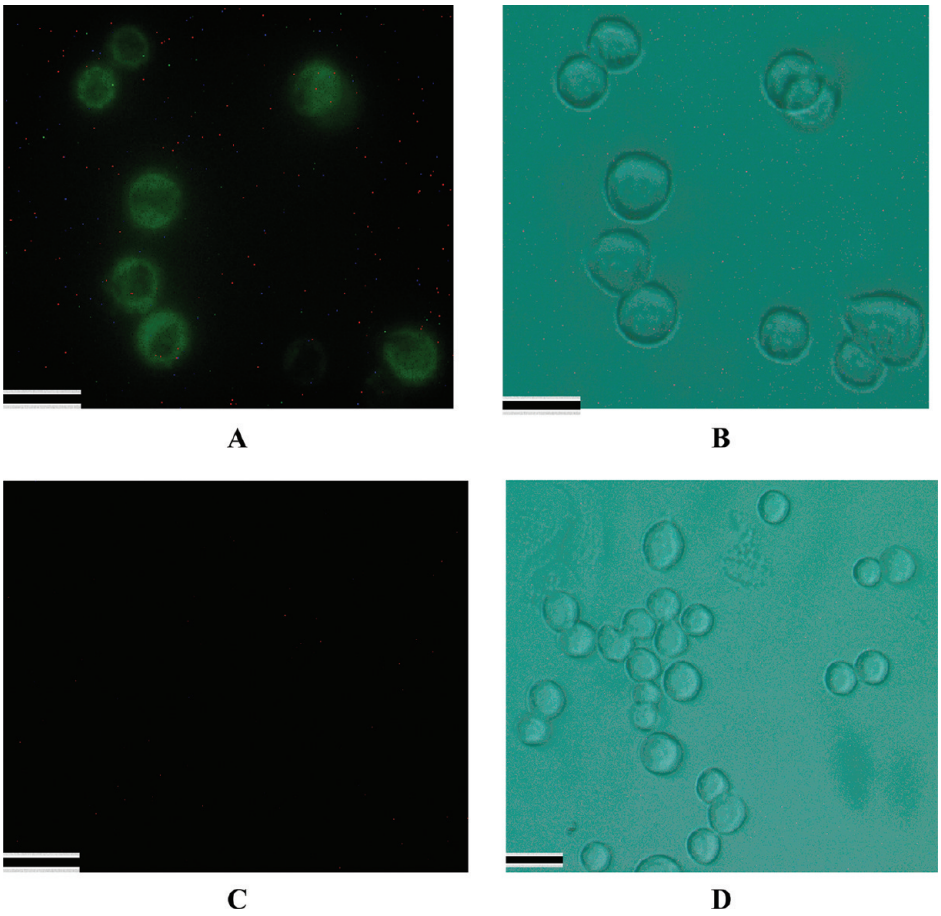

Figure 5. SK-BR-3 cancer cell fluorescent images after incubation with Cy3 modified S6 aptamer attached GNPOP modified SWCNT for an hour. Green indicates the presence of Cy3 labeled nanomaterial on the cell. (B) Bright-field image of SK-BR-3 cells after incubation with Cy3-modified, S6 aptamer-attached, GNPOP-modified SWCNT. (C) MDA-AB cell fluorescent images after incubation with Cy3-modified, S6 aptamer-attached GNPOP modified SWCNT for 4 h. No green fluorescence was observed. (D) Bright-field image of MDA-AB cells after incubation with Cy3-modified, S6 aptamer-attached, GNPOP-modified SWCNT. Scale bar represents 20 μm.

then we have performed MTT test for cell viability. We have not found any cytotoxicity even after 24 h incubation, which shows that our hybrid nanomaterial is highly biocompatible. Carbon nanotubes or gold nanoparticles are known to be capable of converting near-infrared radiation to vibrational energy, to generate sufficient heat for cancer cell killing.[8−15,24−40,51] In our nanotherapy experiment, we have used (1−3) W/cm^2 power 785 nm NIR light for 10 min using a 785 nm OEM laser. Because biological systems mostly lack chromophores that absorb in the NIR light range of 700−1100 nm, use of 785 nm for therapy is very useful for the induction of hyperthermia. SWCNTs are very suitable for photothermal therapy material, due to their strong optical absorbance in the near-infrared (700−1100 nm) region, which is originated from the electronic transitions from the first or second van Hove singularities.[24−42] Because Van Hove-like singularity in the density of states moves toward the top of the valence band, it enhances the effective DOS near the Fermi energy.[24−42] As a result, there is an increase in the electron−phonon interaction and thereby increasing the temperature of the nanotubes.[24−42] Similarly during photothermal therapy, the light absorbed by the gold nanoparticles is transferred to the aptamer and cell environment by rapid electron−phonon relaxation in the nanoparticle followed by phonon−phonon relaxation.[8,11−15,51] As shown in Figures 7 and 8, exposure to the 785 nm light with 1.5 W/cm^2 power for 10 min, caused photo destruction of whole SK-BR-3 breast cancer cells. After therapy, cell viability was detected by MTT test as well as using bright-field inverted microscope techniques.

To find out the amount of cell death, we added trypan blue after NIR radiation exposure. Living cells can not bind with trypan blue and keep themselves colorless. On the other hand, dead cells will bind with the blue dye. As a result, the cell viability can be qualitatively determined from the color of the cell monolayer. As shown in Figure 7B, more than 95% of cancer cells are dead after 10 min of nanotherapy process. Our bright-field inverted microscope image also shows that cancer cells are deformed during nanotherapy process. This cell death following nanoparticle exposure to NIR radiation could be due to numerous factors, including nanoparticle explosion, shock waves, bubble formation, and thermal disintegration.[8−15,24−42] To understand the advantages of using hybrid nanoparticle instead of only GNPOP or only SWCNT, we have also performed photothermal experiment using S6 aptamer -conjugated GNPOP and S6 aptamer-conjugated SWCNT, separately. As shown in Figure 8A, hybrid nanomaterial kills more than 95% of cells even at 1.5 W/cm^2 power of 785 nm light for only 10 min exposure. On the other hand, we need to use about double the power (3 W/cm^2) in the case of only GNPOP to kill the same amount of SK-BR-3 cells.

Our experimental results clearly show that the photothermal effect with hybrid nanoparticle is much more effective and needs much lower power. And it is mainly due to two facts, as follows. (1) In the case of the hybrid nanoparticle, both SWCNT and gold nanoparticle can generate the heat and the amount of heat generation is expected to be the highest for the hybrid nanoparticle than for only SWCNT or for only nanoparticle; and (2) after attachement with cancer cells through S6 aptamer, hybrid nanoparticle has very strong absorption peak at 785 nm, as shown in Figure 4C. Absorption intensity at 785 nm is lower in case of GNPOP attached SK-BR-3 cell and it is minimum in case of S6 aptamer-modified, SWCNT-attached SK-BR-3 cell.

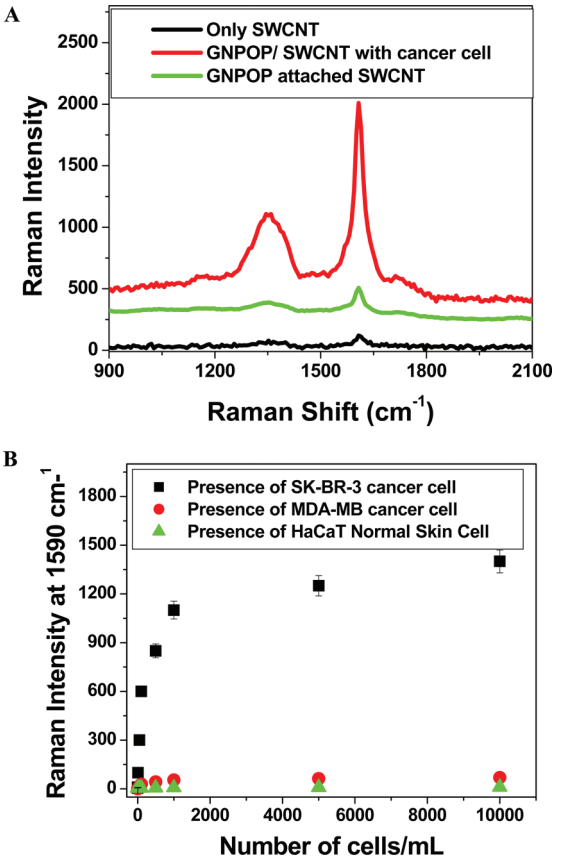

Figure 6. (A) Plot showing SERS enhancement in the presence of 10^4 cells/mL SK-BR-3 breast cancer cell. (B) Plot showing SERS scattering intensity change at 1590 cm^{-1} upon the addition of different concentrations (number of cells/mL) of SK-BR-3, MDA-MB human breast cancerous and HaCaT normal skin cells to S6 aptamer-conjugated, GNPOP-attached SWCNTs. In all cases, we have used 10 μg/mL SWCNT and 10 μg/mL SWCNT hybrid.

Next, to understand how the temparature rises during photothermal therapy, we have performed thermal imaging at every minute interval during therapy process using MikroShot Camera. As shown in Figure 8C, the temparature increases by about 60 °C, when 785 nm laser with 1.5 W/cm^2 power has been exposed to hybrid nanomaterial attached cancer cells. On the other hand, in the same condition, temparature increases only 40 °C, in the case of only SWCNT attached cancer cell and 30 °C for cancer cell without any nanoparticle. Now to demonstrate that our photothermal therapy is highly selective, we have also performed the same photothermal experiment with HER2 negative MAD-MB breast cancer cell and HaCaT normal cell after binding with S6 aptamer atatched hybrid nanoparticle. All the cells were treated using 1.5 W/cm^2 785 nm light for 15 min. As shown in Figure 8B, our time interval cell viability test indicates that within 10 min, most of the SK-BR-3 cancer cells have been killed. On the other hand, cell viability is more than 88% in case of MDA-MB and 95% for HaCaT cell. When light of appropriate wavelength is absorbed by gold nanoparticles, it is converted into heat by rapid electron−phonon relaxation followed by phonon−phonon relaxation.[8−15,24−42] This highly localized heat generated by hybrid nanomaterials will transfer to the cancer cell when hybrid nanoparticles are conjugated with cancer cells and will be able to kills cancer cell. Since photothermal therapy is highly localized therapy, conjugation of hybrid nanomaterials with cancer cell is necessary. As shown in Figures 4B and 5, aggregation of hybrid nanomaterial on cell membranes only occurs in case of HER2 positive SK-BR-3 cells. As a result, photothermal therapy effect should be highly efficient in the presence of SK-BR-3 cell in comparison to MDA-AB and HaCaT cell. Now since hybrid nanomaterials have some absorption at 785 nm light, in the presence of 785 nm light, it will generate some heat, but the heat will be transferred to the solvent, because of the lack of conjugation between hybrid nanomaterial and MDA-AB and HaCaT cell. As we have mentioned before, after incubation, the cell monolayer in the wells was repeatedly rinsed with PBS

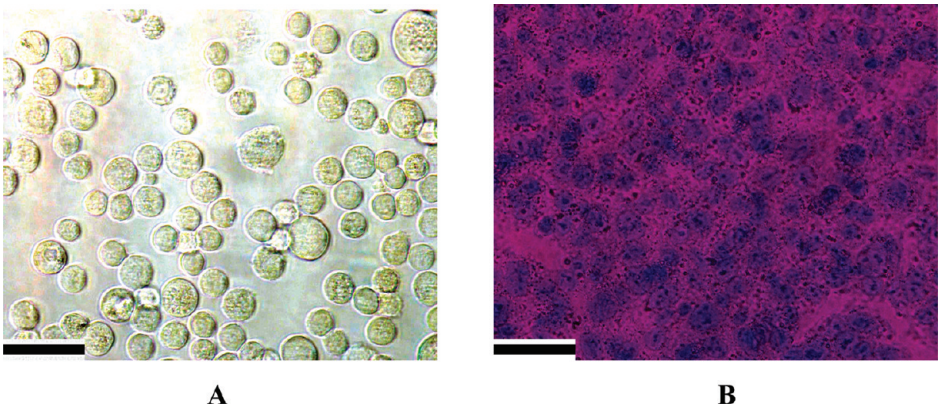

Figure 7. (A) Bright-field inverted microscope images of aptamer-conjugated hybrid nanomaterial-attached SK-BR-3 breast cancer cells stained with trypan blue, before irradiation. (B) Bright-field inverted microscope images after irradiation with 785 nm light with power 1.5 W/cm^2 for 10 min followed by staining with trypan blue. Scale bar represents 20 μm.

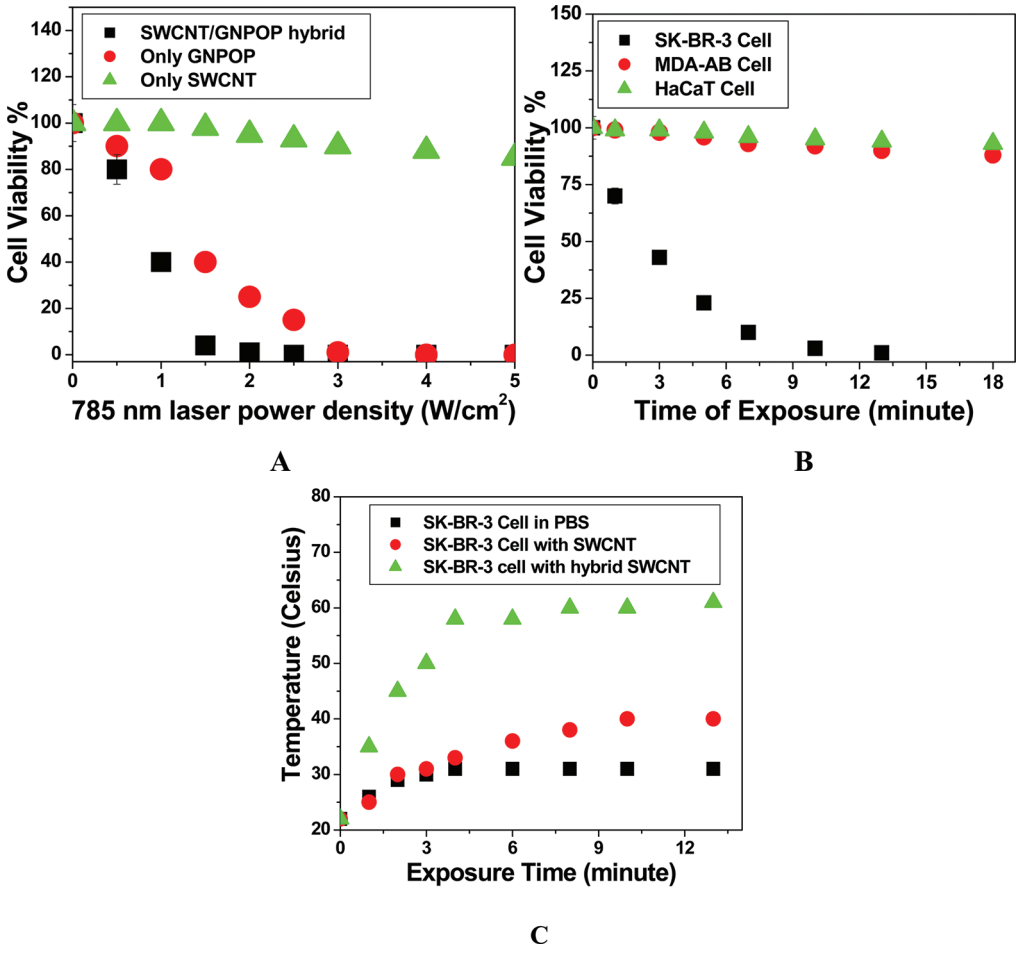

Figure 8. (A) Plot showing 785 nm laser power dependent cell viability for hybrid nanomaterials and its comparison to only GNPOP and only SWCNT. They have been exposed to785 nm laser for 10 min in each case. We have used 100 μg/mL SWCNT, 100 μg/mL hybrid SWCNT, and 1.5 nM GNPOP, to make sure that the amount of GNPOP is the same for SWCNT hybrid and only nanoparticle. (B) Plot showing cell viability measurement when S-6 aptamer attached hybrid nanomaterial conjugated SK-BR-3, MDA-MB, and HaCaT cells were treated using 1.5 W/cm^2 785 nm light for 15 min. (C) Plot showing photothermal heating curves during therapy process, when 785 nm laser with 1.5 W/cm^2 power has been exposed for 15 min.

buffer to remove the nonspecifically adsorbed nanomaterial remaining in the medium and then exposed to the laser at 785 nm. As a result, the amount of nanomaterial present in the medium will be very low. For this reason, the effective temperature increase in cancer cells will be low, which will not be enough to kill the cells.

CONCLUSIONS

In conclusion, in this manuscript, we have demonstrated for the first time chemical design of aptamer-conjugated, hybrid-nanomaterial-based SERS probe for targeted diagnosis of SK-BR-3, human cancer cells even at 10 cancer cells/mL level. We have shown that in the presence of targeted human cancer cell, aptamer-conjugated hybrid nanomaterial provides a significant enhancement of the Raman signal intensity of SWCNT D and G bands by 3 orders of magnitude. Our experimental data with HER2 negative MDA-MB breast cancer and HaCaT normal skin cell lines clearly demonstrate that our SERS assay is highly sensitive to targeted human breast cancer cell and it will be able to distinguish from other nontargeted cancer cell lines. Current SERS probe is free from dye labeling and as a result, this SERS assay will not suffer from photo bleaching problem. We have also shown that during photothermal therapy of S6 aptamer conjugated hybrid nanomaterials attached SK-BR-3 cancerous cells, the localized heating that occurs due to the absorption of 785 nm continuous NIR irradiation, is able to cause irreparable cellular damage and kills selectively most of the cancerous cells within 10 min at 1.5 W/cm^2 power. This hybrid nanotechnology based assay is rapid, takes about 20 min from cancer cell binding to detection and destruction of the cell. Our data show that photothermal response for hybrid nanomaterial is far better than single nanomaterial. After optimization of different parameters, we believe that this hybrid nanotechnology driven assay could have enormous potential application in rapid detection and photothermal therapy of clinical samples.

AUTHOR INFORMATION

Corresponding Author

*E-Mail: paresh.c.ray@jsums.edu. Fax: 601-979-3674.

ACKNOWLEDGMENT

Dr. Ray thanks NIH-SCORE Grant S06GM 008047 and NSF-PREM Grant DMR-0611539 for their generous funding. We also thank all the reviewers for their valuable suggestions, which improved the quality of the manuscript significantly.

REFERENCES

(1) Bray, F.; Møller, B. *Nat. Rev. Cancer* **2006**, *6*, 63.
(2) Brindle, K. *Nat. Rev. Cancer* **2008**, *8*, 94.
(3) Fang, X.; Tan., W. *Acc. Chem. Res.* **2010**, *43*, 48.
(4) Choi, C. H. J.; Alabi, C. A.; Webster, P.; Davis, M. E. *Proc. Natl. Acad. Sci. U.S.A.* **2010**, *107*, 1235.
(5) Zheng, X.; Xing, D.; Zhou, F.; Wu, B.; Chen, W. R. *Mol. Pharmaceutics* **2011**, *8*, 447.
(6) Chen, H. Z.; Tsai, S. Y.; Leone, G. *Nat. Rev. Cancer* **2009**, *9*, 785.
(7) Sarkar, B.; Dosch., J.; Simeone, D. M. *Chem. Rev.* **2009**, *109*, 3200.
(8) Lu, W.; Singh, A. K.; Khan, S. A.; Senapati, D.; Yu, H.; Ray, P. C. *J. Am. Chem. Soc.* **2010**, *132*, 18103.
(9) Ferrari, M. *Nat. Rev. Cancer* **2005**, *5*, 161.
(10) Scheinberg, D. A.; Villa, C. H.; Escorcia, F. E.; McDevitt, R. M. *Nat. Rev. Clinic. Oncol.* **2010**, *7*, 266.
(11) Jain, P. K.; Huang, X.; El-Sayed, I. H.; El-Sayed, M. A. *Acc. Chem. Res.* **2008**, *41*, 1578.
(12) King, S. H.; Huh, Y. M.; Kim, S.; Lee, D.-K. *Bull. Korean Chem. Soc.* **2009**, *30*, 1827.
(13) Fang, X.; Tan, W. *Acc. Chem. Res.,.* **2010**, *43*, 48.
(14) Lal, S.; Clare, S. E.; Halas, N. J. *Acc. Chem. Res.* **2008**, *41*, 1842.
(15) Peer, D.; Karp, J. M.; Hong, S.; Farokhzad, O. C.; Margalit, R.; Langer, R. *Nat. Nanotechnol.* **2007**, *2*, 751–760.
(16) Giljohann, D. A.; Mirkin, C. A. *Nature* **2009**, *462*, 461.
(17) Yong, K. T.; Hu, R.; Roy, I.; Ding, H.; Vathy, L. A.; Bergey, E. J.; Mizuma, M.; Maitra., A.; Prasad, P. N. *ACS Appl. Mater. Interfaces* **2009**, *1*, 710.
(18) Kumar, R.; Ohulchanskyy, T. Y.; Roy, I.; Gupta, S. K.; Borek, C. T.; Prasad, P. N. *ACS Appl. Mater. Interfaces* **2009**, *1*, 1474.
(19) Jang, B.; Kim, Y. S.; Choi, Y. *Small* **2011**, *7*, 265.
(20) Sanpui, P.; Chattopadhyay, A.; Ghosh, S. S. *ACS Appl. Mater. Interfaces* **2011**, *3*, 218.
(21) Schuller, J. A.; Barnard, E. S.; Ca., W.; Jun, Y. C.; White, J. S.; Brongersma, M. L *Nat. Mater.* **2010**, *9*, 193.
(22) Yong, K. T.; Ding, H.; Roy, I.; Law, W. C.; Bergey, E. J.; Maitra., A.; Prasad, P. N. *ACS Nano* **2009**, *3*, 502.
(23) Kennedy, L. C.; Bickford., L. R.; Lewinski., N. A.; Coughlin., A. J.; Hu, Y.; Day, E. S.; West, J. L.; Drezek, R. A. *Small* **2011**, *7*, 169.
(24) Bhirde, A. A.; Patel, V.; Gavard, J.; Zhang, G.; Sousa, A. A.; Masedunskas, A.; Leapman, R. D.; Weigert, R.; Gutkind, S. J.; Rusling, J. F. *ACS Nano* **2009**, *3*, 307.
(25) Duque, J. G.; Cognet, L.; Parra-Vasquez, A. N. G.; Nicholas, N.; Schmidt, H. K.; Pasquali, M. *J. Am. Chem. Soc.* **2008**, *130*, 2626.
(26) Gethard, K.; Sae-Khow, O.; Mitra, S. *ACS Appl. Mater. Interfaces* **2011**, *3*, 110.
(27) Dan, B.; Irvin, G. C.; Pasquali, M. *ACS Nano* **2009**, *3*, 835.
(28) Behabtu, N.; Lomeda, J.; Green, M. J.; Higginbotham, A. L.; Sinitskii, A.; Kosynkin, D. K.; Tsentalovich, D.; Parra-Vasquez, A. N. G.; Schmidt, J.; Kesselman, E. *Nat. Nanotechnol.* **2010**, *5*, 406.
(29) Bachilo, S. M.; Strano, M. S.; Kittrell, C.; Hauge, R. H.; Smalley, R. E.; Weisman, R. B. *Science* **2002**, *298*, 2361.
(30) Lin, Y.; Zhang, L.; Yao, W.; Qian, H.; Ding, D.; Wu, W.; Jiang, X. *ACS Appl. Mater. Interfaces* **2011**, *3*, 995.
(31) Ashwin, A. B.; Vyomesh, P.; Julie, G.; Guofeng, Z.; Alioscka, A. S.; Andrius, M.; Richard, D. L.; Roberto, W. J.; Silvio, G.; James, F. R. *ACS Nano* **2009**, *3*, 307.
(32) Xiang, J.; Drzal, L. T. *ACS Appl. Mater. Interfaces* **2011**, *3*, 1325.
(33) Kolosnjaj, T. J.; Hartman, K B.; Boudjemaa, S.; Ananta, J. S.; Morgant, G.; Szwarc, H.; Wilson, L. J.; Moussa, F. *ACS Nano* **2010**, *4*, 1481.
(34) Poland, C. A.; Duffin, R.; Kinloch, I.; Maynard, A.; Wallace, W. A.; Seaton, A.; Stone, V.; Brown, S.; Macnee, W.; Donaldson, K. *Nat. Nanotechnol.* **2008**, *3*, 423.
(35) Chen, J.; Chen, S.; Zhao, X.; Kuznetsova, V. L.; Wong, S. S.; Ojima, I. *J. Am. Chem. Soc.* **2008**, *130*, 16778.
(36) Kostarelos, K.; Bianco, A.; Prato, M. P. *Nat. Nanotechnol.* **2009**, *4*, 627.
(37) Liu, Z.; Fan, A.; Rakhra, K.; Sherlock, S.; Goodwin, A.; Chen, X.; Yang, Q.; Felsher, D.; Dai, H. *Angew. Chem., Int. Ed.* **2009**, *48*, 7668.
(38) Kam, N. W. S.; Connell, M. O.; Wisdom., J. A.; Dai., H. J. *Proc. Natl. Acad. Sci. U.S.A.* **2005**, *102*, 11600.
(39) Khanderi, J.; Hoffmann, R. C.; Engstler., J.; Schneider., J. J.; Arras., J.; Claus, P.; Cherkashinin, G. *Chem.—Eur. J.* **2010**, *16*, 2300.
(40) Stern, J. M.; Stanfield, J.; Hsieh, J. T.; Cadeddu, J. A. *J. Urology* **2007**, *177*, 210.
(41) Kumar, R.; Aykol, M.; Cronin, S. B. *Phys. Rev. B* **2008**, *78*, 165428.
(42) Wu, G.; Zhou, J.; Dong, J. *Phys. Rev. B* **2005**, *72*, 115411.
(43) Qian, X.; Zhou, X.; Nie, S. *J. Am. Chem. Soc.* **2008**, *130*, 14934.
(44) Wang., L.; Li, H.; Tian, J.; Sun, X. *ACS Appl. Mater. Interfaces* **2010**, *2*, 2987.
(45) Dasary, S. S. R.; Singh, A. K.; Senapati., D.; Yu, H.; Ray, P. C. *J. Am. Chem. Soc.* **2009**, *131*, 13806.
(46) Camden, J. P.; Dieringer, J. A.; Zhao, J.; Van Duyne, R. P. *Acc. Chem. Res.* **2008**, *41*, 1653.
(47) Brus, L. *Acc. Chem. Res.* **2008**, *41*, 1742.
(48) Pallaoro, A.; Braun, G. B.; Reich, N. O.; Moskovits, M. *Small* **2010**, *6*, 618.
(49) Su, Y.; He, Q.; Yan, X.; Fei, J.; Cui, Y.; Li, J. *Chem.—Eur. J.* **2011**, *17*, 3370.
(50) Kang, T.; Yoo., M. S.; Yoon., I.; Lee., S.; Choo., J.; Lee, S. Y.; Kim, B. *Chem.—Eur. J.* **2011**, *17*, 2211.
(51) Huang, X.; El-Sayed, I. H.; Qian, W.; El-Sayed, M. *J. Am. Chem. Soc.* **2006**, *128*, 2115.
(52) Lu, W.; Arumugam, S. R.; Senapati., D.; Singh, A. K.; Arbneshi, T.; Khan, S. A.; Yu, H.; Ray, P. C. *ACS Nano* **2010**, *4*, 1739.
(53) Xuan, S.; Wang, F.; Josie, M. Y.; Lai, K. W. Y.; Sham, Y.; Xiang, J.; Wang, S. F.; Lee, J C.; Christopher, H. K.; Ken, C. F L. *ACS Appl. Mater. Interfaces* **2011**, *3*, 237.
(54) Ray, P. C. *Chem. Rev.* **2010**, *110*, 5332.
(55) Beqa, L.; Singh, A. K.; Khan, S. A.; Senapati, D.; Arumugam, S. R.; Ray, P. C. *ACS Appl. Mater. Interfaces* **2011**, *3*, 668.
(56) Neely, A.; Perry, C.; Varisli, B.; Singh, A. K.; Arbneshi, T.; Senapati, D.; Kalluri, J. R.; Ray, P. C. *ACS Nano* **2009**, *3*, 2834.
(57) Singh, A. K.; Senapati, D.; Wang, S.; Griffin, J.; Neely, A.; Candice, P.; Naylor, K M.; Varisli, B.; Kalluri, J. R.; Ray, P. C. *ACS Nano* **2009**, *3*, 1906.
(58) Griffin, J.; Singh, A. K.; Senapati, D.; Lee, E.; Gaylor, K. B. J J.; Ray, P. C. *Small* **2009**, *5*, 839.
(59) Griffin, J.; Singh, A. K.; Senapati., D.; Rhodes, P.; Mitchell, K.; Robinson, B.; Yu, E.; Ray, P. C. *Chem.—Eur. J.* **2009**, *15*, 342.
(60) Darbha, G. K.; Rai, U. S.; Singh, A. K.; Ray., P. C. *J. Am. Chem. Soc.* **2008**, *130*, 8038.
(61) Griffin, J.; Ray, P. C. *J. Phys. Chem. B. (Letter)* **2008**, *112*, 11198.
(62) Darbha, G. K.; Rai., U. S.; Singh, A. K.; Ray, P. C. *Chem.—Eur. J.* **2008**, *14*, 3896.
(63) Kang, T.; Yoo, M. S.; Yoon., I.; Lee., S.; Choo, J.; Lee, S. Y.; Kim, B. *Chem.—Eur. J.* **2011**, *17*, 2211.
(64) Hayashi, K; Ono, K. H. S.; Makoto, S.; Makoto, M.; Wataru, S.; Toshinobu, Y. *ACS Appl. Mater. Interfaces* **2010**, *2*, 1903.
(65) Darbha, G. K.; Ray., A.; Ray, P. C. *ACS Nano* **2007**, *3*, 208.
(66) Tiwari, S. V.; Oleg., T.; Darbha, G. K.; Hardy, W.; Singh, J. P.; Ray, P. C. *Chem. Phys. Lett.* **2007**, *446*, 77.
(67) Ray, P, C. *Angew. Chem., Int. Ed.* **2006**, *45*, 1151.
(68) Wang, S.; Singh, A. K.; Senapati., D.; Neely, A.; Yu, H.; Ray, P. C. *Chem.—Eur. J.* **2010**, *16*, 5600.
(69) Hao, F.; Nehl, C. L.; Hafner, J. H.; Nordlander, P. *Nano Lett.* **2007**, *7*, 729.
(70) Song, H. M.; Wei, Q.; Ong, Q. K.; Wei, A. *ACS Nano* **2010**, *6*, 5163.
(71) Kim, K.; Lee, H, S. *J. Phys. Chem. B* **2005**, *109*, 18929.
(72) Chen, J.; Hamon, M. A.; Hu, H.; Chen, Y.; Rao, A. M.; Eklund, P. C.; Haddon, R. C. *Science* **1998**, *282*, 95.